Development of a Wide Dynamic Range Neutron Flux Measurement Instrument Having Fast Time Response for Fusion Experiments

Daijiro ITO, Hiroyuki YAZAWA, Makoto TOMITAKA, Tsuyoshi KUMAGAI, Shigehiro KONO, Michinori YAMAUCHI, Tsuyoshi MISAWA[1)], Takashi KOBUCHI[2)], Hiroshi HAYASHI[2)], Hitoshi MIYAKE[2)], Kunihiro OGAWA[2,3)], Takeo NISHITANI[2)] and Mitsutaka ISOBE[2,3)]

Toshiba Energy Systems & Solutions Corporation, Fuchu 183-8511, Japan
[1)]*Institute for Integrated Radiation and Nuclear Science, Kyoto University, Sennan-gun, Osaka 590-0494, Japan*
[2)]*National Institute for Fusion Science, National Institutes of Natural Sciences, Toki 509-5292, Japan*
[3)]*The Graduate University for Advanced Studies, SOKENDAI, Toki 509-5292, Japan*

(Received 7 October 2020 / Accepted 15 December 2020)

A wide-range neutron flux measurement instrument is developed herein for monitoring the total neutron emission rate and yield of the Large Helical Device (LHD) during deuterium experiments implemented from March 2017 in the National Institute for Fusion Science (NIFS), Japan. The instrument is designed for and installed on the Neutron Flux Monitoring (NFM) system, which measures the counting rate using a ^{235}U Fission Chamber. By combining the pulse counting and Campbell methods, the Digital Signal Processing Unit (DSPU) realized a wide dynamic range of over six orders of magnitude from 1×10^3 counts/s (cps) to 5×10^9 cps. This study explains and discusses how the instrument is developed, including topics from the predevelopment activities to the verification test at the Kyoto University Critical Assembly (KUCA). Experimental results in the LHD using the finished products suggest that the NFM system works well during deuterium experiments.

Keywords: neutron flux measurement, fission chamber, wide dynamic range, fast time response, Campbell method, Kyoto University Critical Assembly, Large Helical Device

DOI: 10.1585/pfr.16.1405018

1. Introduction

Generally a method using the fission chamber and combining the pulse counting and the Campbell methods (hereinafter referred to as "Pulse/Campbell method") is used to measure neutron flux over a wide range. This method has been conventionally applied to in-core nuclear reactor instrumentation for nuclear power plants and neutron monitoring systems in nuclear facilities [1].

In fusion experimental facilities, such as the LHD, measuring temporal changes in the total neutron emission rate (S_n) is necessary when studying the physics of plasma and controlling of fusion power. Particularly, when a wide range measurement is required, it is appropriate to apply the Pulse/Campbell method.

When the Pulse Campbell method is applied to fusion experiments, fast time responsiveness that is several orders of magnitude higher than in-core instrumentation is required. In developing an instrument with fast time responses, the following two points should be focused on: statistical accuracy of measured values and electromagnetic noise sensitivity. Referring to the experimental results of JT-60 to which an equipment of this measuring method was applied, it was found that the equipment designed for the fusion experiment considering the fast time response was easily affected by electromagnetic noises [2].

The LHD is one of the large experimental devices developed for research on helical fusion reactors. An important objective of the LHD is to improve the technology of high energy ion confinement [3]. Measurement of S_n is indispensable for this object. For contributing to the success of LHD experiments, we have applied digital signal processing technology and have developed the new instrument with an improved noise tolerance function.

2. Requirements and Basic Design Policies

During the deuterium experiment in the LHD, the S_n is an index that provides important information for the study of high-energy ion confinement. In this experiment, S_n changes widely and rapidly depending on the plasma heating pattern. The maximum S_n in the experiment is predicted to be 1.9×10^{16} neutrons/s upon attaining the full power [4]. Moreover, the S_n during the experiment changes on a fast time scale of approximately several 10 ms [5].

Therefore, the NFM system must realize high-

author's e-mail: daijiro.ito@toshiba.co.jp

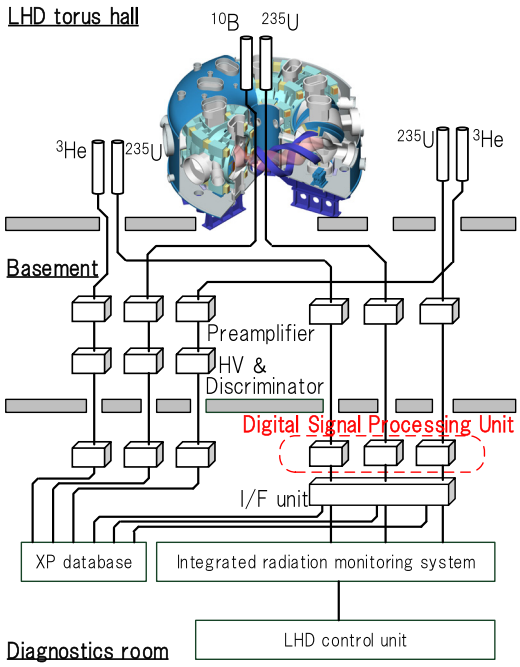

Fig. 1 NFM system overview.

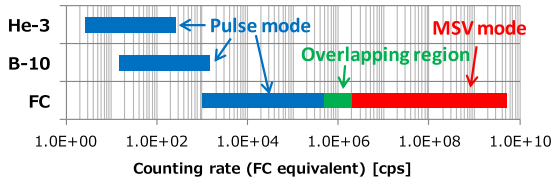

Fig. 2 Measurement range of each detector.

precision neutron measurements with a fast time constant and wide dynamic range. Figure 1 shows a schematic overview of the NFM system. This system comprises several types of neutron detectors covered with neutron moderators, and each type of detector has a different neutron sensitive material to yield different sensitivities. In the area wherein the emission rate of neutrons is relatively small, ^{3}He and ^{10}B neutron detectors are used in combination with counters that have a dynamic range of approximately two orders of magnitude. Furthermore, in other area with a relatively high emission rate, a ^{235}U fission chamber having a neutron sensitivity lower than that of the above detector is used to realize a comprehensive high-dynamic-range measurement, as shown in Fig. 2. Primary requirements and basic design policies for the ^{235}U system are shown in Secs. 2.1-2.3.

2.1 Wide dynamic range

The maximum neutron flux at the detector position is estimated as 10^{10} nv [5]. Moreover, the detector sensitivity specification is 0.1 cps/nv [5]. From these values, the predicted value of the maximum counting rate is $10^{10} \times 0.1 = 10^{9}$ cps [5] (Table 1). In the case of normal

Table 1 Expected maximum counting rate.

Items	Values
Total neutron emission rate (S_n)	1.9×10^{16} n/s
Neutron flux at detector position	$\sim 10^{10}$ nv
Detector sensitivity	0.1 cps/nv
Maximum counting rate	10^{9} cps
Measurable maximum counting rate (safety ratio is 5)	5×10^{9} cps

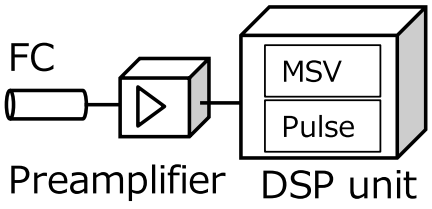

Fig. 3 Single channel block diagram.

pulse counting, the 10^{9} cps is an extremely high counting rate and simply counting pulse signals coming from the detector cannot help the measurements owing to pileup. In such a case, the Campbell method, which is based on a simple equation expressed as Eq. (1) [6], should be used. This equation implies that the mean square value (MSV) of signal fluctuation is proportional to the number of neutrons.

$$\langle I^2\rangle - \langle I\rangle^2 = \langle N\rangle \int_0^\infty [i(t)]^2 dt, \tag{1}$$

$\langle I^2\rangle - \langle I\rangle^2$: Variance in the current from a source of random current pulses
$\langle N\rangle$: Average pulse rate
$[i(t)]$: Pulse height
t : Time

However, the Campbell method has a large fluctuation at a low count rate and is not suitable for measurements of a low count rate as opposed to pulse counting. Consequently, with the aim of realizing a wide dynamic range, the signal of one detector must be processed by a combination of the pulse counting and the Campbell methods. Figure 3 shows a simple system block diagram for a channel. The preamplifier amplifies the detector signal. The Digital Signal Processing Unit (DSPU), which has the processing circuits for the pulse counting and the Campbell methods, processes the signal from the preamplifier.

Furthermore, as the upper limit of the counting rate that can be actually measured using the pulse counting method is of the order of 10^{6} cps, it is necessary to measure the range of 10^{6} cps to 5×10^{9} cps using the Campbell method, as shown in Table 2. Normally, the dynamic range of a single measurement circuit is at the most approximately two orders of magnitude owing to constraints such as A/D converters and circuit noise. Accordingly, as

Table 2 Measurement modes.

Measurement mode	Counting rate range
Pulse counting	10^3 to ~ 10^6 cps
Campbell	~ 10^6 to ~5×10^9 cps

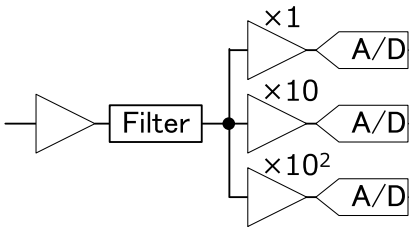

Fig. 4 Basic circuit schematic for the Campbell method.

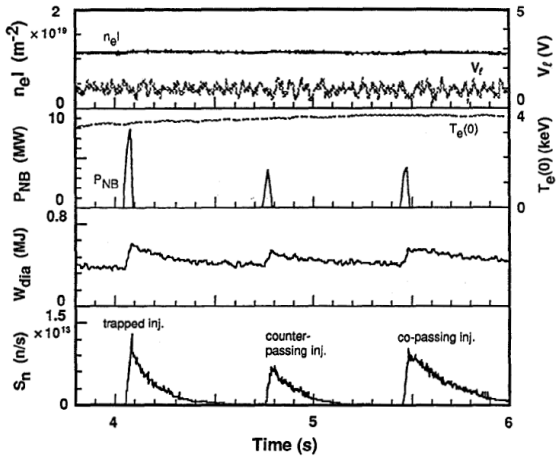

Fig. 5 Total neutron emission rate in the NB-blip experiment. Reproduced with permission from K. Tobita *et al.*, Nucl. Fusion **34**, No. 8, 1097 (1994) [3]. P_{NB} is a short pulse neutral beam injection. S_n is neutron emission rate as a response of the injected beam.

shown in Fig. 4, the signal is branched into three systems, and the measurement ranges of the respective systems are shifted so that a wide measurement range is obtained.

2.2 Fast time response

The NFM system requires a fast time response to accurately capture the behavior of neutron flux that changes rapidly and dynamically. One approach to evaluate fast ion confinement in deuterium experiments is to irradiate a pulsed neutral particle beam and then measure the response of the S_n (referred to as "NB-blip"). In this NB-blip experiment, the S_n changes on a time scale of approximately several tens of ms. Figure 5 shows an example of a past NB-blip experiment performed in JT-60U [3].

If the time response of the measurement is not sufficiently fast for the above time scale, the response of the measured S_n is affected by the characteristics of the signal

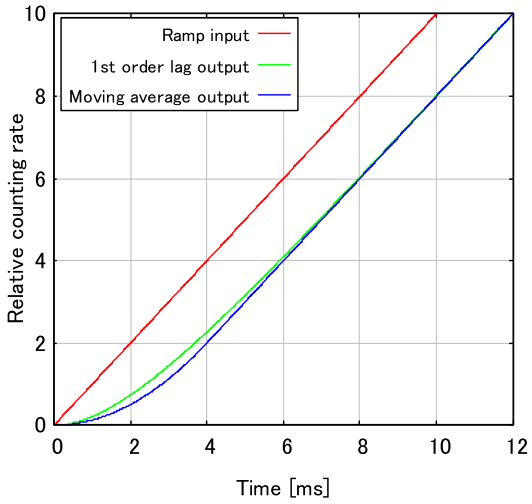

Fig. 6 Comparison of the 1st order lag and moving average response.

processor. Then it transforms into a dull waveform that is different from the change in the actual S_n. To avoid this, the signal processing system requires a fast time response of approximately 10 times or more with respect to the time scale in which the signal source to be measured fluctuations. Based on this point of view, the NFM system required a time response equivalent to a 1st order lag time constant of 2 ms.

In general, in control engineering, an appropriate and simple input is assumed to understand the response characteristics of a signal processing process. When considering the response characteristics of a neutron measurement instrument, it is appropriate to consider the response to a ramp-like input in which the signal changes at a constant rate, called ramp response because the temporal change in the signal source itself is slower than the signal processing time scale. The unit ramp response of the first-order lag can be expressed as Eq. (2). Equation (2) shows that when sufficient time has elapsed, a waveform delayed by a time constant τ from the input waveform can be obtained as the output.

$$f(t) = t - \tau\left(1 - e^{-\frac{t}{\tau}}\right), \tag{2}$$

$f(t)$: Response of 1st order lag
τ : Time constant

Conversely, the delay time of the moving average with respect to the ramp-shaped input is $T_m/2$ if the moving average time is T_m. That is, if the moving average time is set such that $T_m/2 = \tau$, the first-order lag and the moving average response can be regarded as equivalent. Therefore, the signal processing parameter is designed to calculate one measurement result in every 0.5 ms processing period and output the measurement result averaged over a moving average time of $T_m = 4$ ms. Figure 6 shows a comparison of the first-order lag when $\tau = 2$ ms and the moving aver-

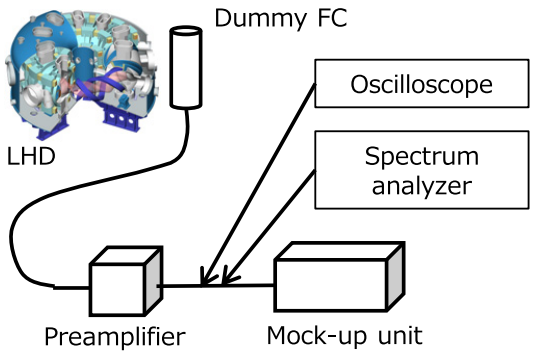

Fig. 7 Preinvestigation setup.

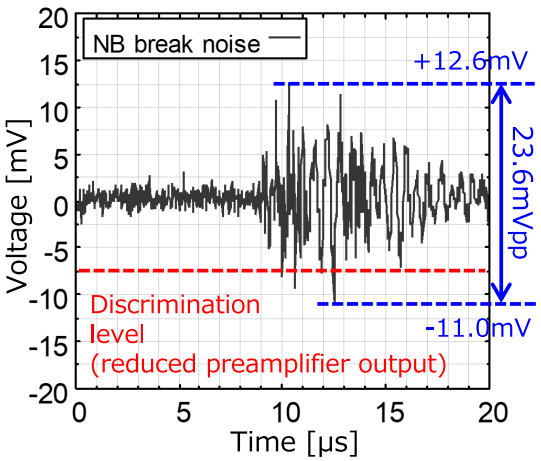

Fig. 8 Noise waveform (preamplifier output).

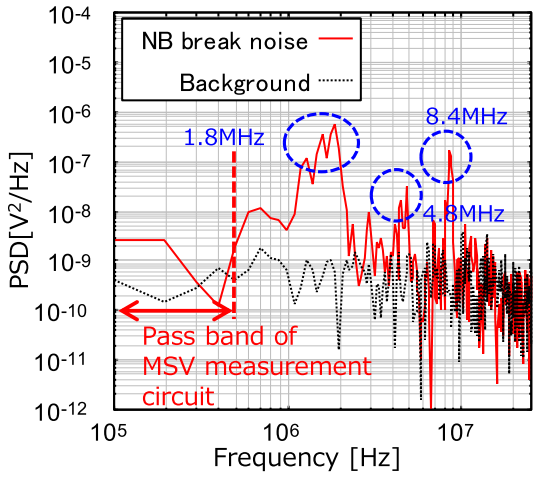

Fig. 9 Distribution of PSD of noise waveform.

age response when T_m = 4 ms. The moving average is a response equivalent to the first order lag.

2.3 Sufficient noise tolerance

The plasma experimental device uses many high-power and control systems in combination for plasma heating and confinement and is driven using a large amount of energy. As a result, there are always sources of noise around the measurement system that often interfere with the measurement. Therefore, the neutron measurement equipment requires a noise tolerance function that is sufficiently robust not to cause fluctuations in measured values owing to noise superposition. In particular, in the case of an equipment with a high-speed response as described in Sec. 2.2, a slightly superimposed noise on the measured value can cause large influence.

In general, in the development of measurement equipment, it is desirable to investigate in advance what type of electromagnetic noise is superimposed in the measurement environment prior to starting the design. By conducting a preliminary survey, it is possible to construct a signal processing function that meets the requirements of neutron measurement and avoids the electromagnetic noise occurring in the installation environment.

With respect to the NFM system, prior to its development, a noise investigation was conducted. We set a temporary measurement system shown in Fig. 7 at the location where the permanent equipment was to be installed at, and we then measured the waveform and frequency spectrum of noise caught by the system.

From this investigation, it was found that when the neutral particle beam (NB) broke down, a single large electromagnetic noise occurred. Figure 8 shows an example of actual waveform measured when this electromagnetic noise is superimposed on the signal waveform. It was found that the noise exhibited a shape that lasted for 10 μs while swinging between positive and negative polarities. This waveform was the output signal of the preamplifier. In this system, the typical amplitude of a pulse wave by ordinary neutron detection was approximately 7.5 mV and the time width was approximately 100 ns, whereas the noise was higher than 10 mV. Thus, the investigation confirmed that noise was larger than the threshold for pulse signal detection and thus affected the measurement result of the count rate obtained through the pulse mode measurement. For example, if an incorrect count was provided 10 times before the noise waveform decayed, a count rate of 10/0.5 ms × 1/8 = 2.5 kcps could be instantaneously measured. This effect was not negligible.

Furthermore, the frequency spectrum is as shown in Fig. 9, and the power spectral density (PSD) in the frequency range from 1 to 10 MHz is relatively large. If the filter circuit for measurement in the Campbell mode included this frequency band, the measurement value obtained using the Campbell mode measurement ought to be affected by the noise.

In response to the above mentioned result of the field survey, special signal processing methods for suppressing the influence of noise were prepared for both the pulse counting and Campbell methods.

One of these special signal processes is to perform a

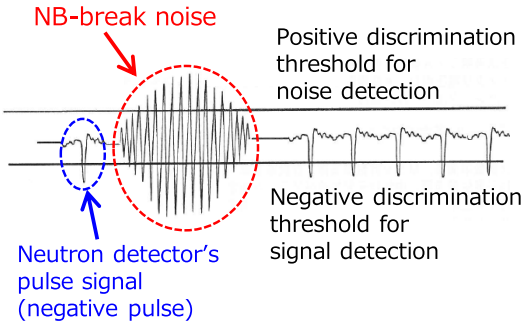

Fig. 10 Schematic diagram of the bipolar discrimination.

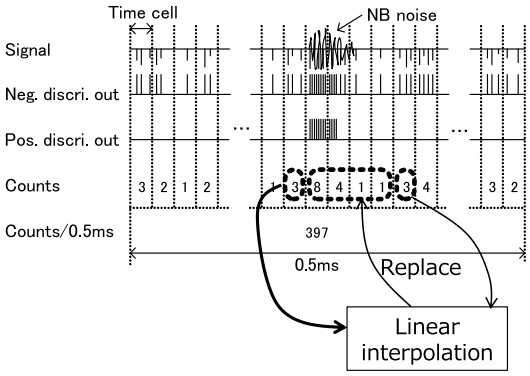

Fig. 11 Noise tolerance function for pulse counting.

short time counting rate correction for the pulse counting method. This method utilizes the fact that the noise is a bipolar waveform and that the duration of the noise is approximately 10 μs, whereas the normal neutron signal is a unipolar pulse.

First, the counting duration for the process to obtain one count rate measurement value is 0.5 ms. However, rather than simply continuing counting for 0.5 ms, the count value of a minute time interval which length is on the order of microseconds is repeatedly measured and the count value of that minute time is integrated until 0.5 ms elapses. Subsequently, as the normal pulse signal is negative and the noise waveform is bipolar, a positive discrimination circuit for noise detection is provided, as shown in Fig. 10. When the positive discrimination threshold is exceeded, it is determined that noise is superimposed on a normal signal. When it is determined, the minute time count values around the noise, which are potentially affected by the noise, are excluded from the integration and replaced with values obtained through linear interpolation with the preceding and succeeding values, thereby suppressing the noise from affecting the count rate. An overview of this process is shown in Fig. 11.

Meanwhile, the noise tolerance function for the Campbell method is to create a low-pass filter having a high-order multistage configuration and a steep high-frequency cutoff characteristic. As shown in Fig. 9, the

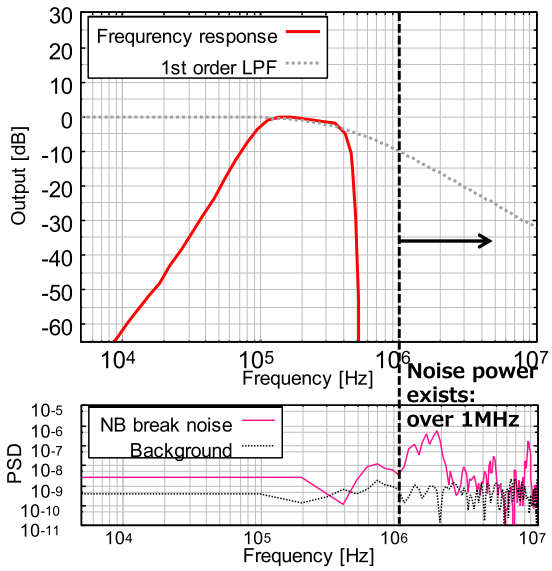

Fig. 12 Frequency characteristics of the band pass filter for the Campbell method.

noise power increased when the frequency exceeded approximately 1 MHz. Therefore, the filter coefficient was designed to create a low-pass filter with a sufficiently large attenuation factor of or greater than 60 dB in the region of MHz or higher. Furthermore, as a low-frequency signal is necessary to calculate the MSV voltage, a high-order filter is applied to create a steep characteristic. Figure 12 shows the frequency characteristics of the designed filter circuit. Actually, the attenuation factor is 60 dB at approximately 500 kHz.

3. Equipment Design of DSPU

3.1 Structure

In accordance with the basic development policy for a wide dynamic range, fast time response, and noise tolerance function as described in Sec. 2, the DSPU was specifically designed. It was designed to be mounted and operated in a standard rack; therefore, it was designed as a 19-inch rack-mount unit at 4U high. Figure 13 shows the appearance of the DSPU. Interfaces such as displays and buttons are arranged on the front side and terminals for power supply and signals are arranged on the back side.

3.2 Signal processing function

Figure 14 represents the block diagram showing signal processing of the DSPU. As shown in Sec. 2.1, the DSPU has the functions of pulse counting and MSV measuring of neutrons over a wide range. The signal processing circuit of the DSPU calculates the pulse count rate and the MSV voltage from the input signal, respectively, and obtains the S_n and yield by combining these two results. This signal processing has the operation period shown in Sec. 2.2. The DSPU is designed to have fast response. Furthermore, the

DSPU has two functions for noise removal, as described in Sec. 2.3.

The measurement values thus obtained are converted into analog signals and digital data, which are outputs to external data acquisition systems. The analog signals are reference outputs for verifying digital data and are voltage signals proportional to the count rates. They comprise the pulse mode count rates divided into two ranges and Campbell mode count rates divided into three ranges, for a total of five outputs. On the other hand, digital data is a data packet that contains Sn value obtained by multiplying the counting rate by a conversion coefficient, a time synchronization flag, and so on. the data is transmitted by the UDP/IP protocol. Owing to the total emission rate being obtained by combining the pulse and the Campbell modes, it is referred to when confirming the linearity between these two modes or when performing the Campbell mode gain calibration. As the Campbell mode value is the MSV voltage, comparing it with the pulse mode data and setting the conversion coefficient to convert the MSV voltage into the counting rate (cps) is necessary. In addition to the S_n, the digital data includes the total neutron emission yield obtained by summing instantaneous value. This is the value to be referred to when making a comparison with a neutron activation foil or the like. Moreover, this value can be reset to zero using the clear button on the DSPU control panel.

The other output signal is a pulse output. This is a TTL level logic pulse that is output each time a pulse signal is detected in a pulse mode circuit. The measured value in pulse mode is calculated from the number of pulses counted in a counting time of 0.5 ms (i.e., one pulse in 0.5 ms corresponds to 2000 cps); therefore, sufficient statistical accuracy cannot be obtained without above a certain number of pulses. Hence, it is necessary to refer to this pulse output when confirming a low count rate of less than 1 cps to several hundred of cps, for example, when performing sensitivity calibration using a radiation source.

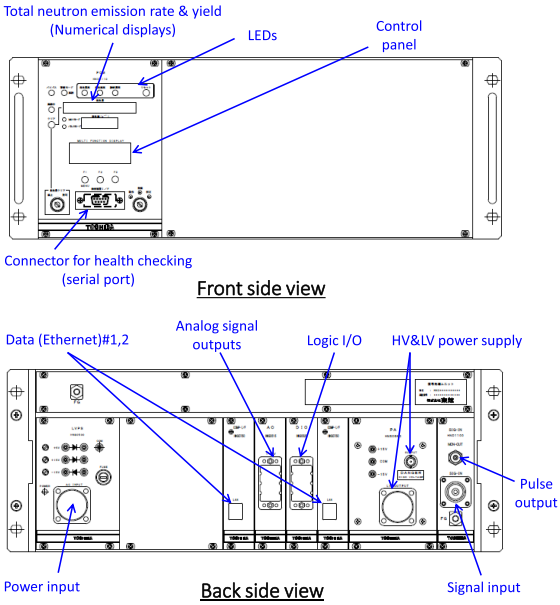

Fig. 13 DSPU external form.

4. Verification

4.1 Concerns about the measurement characteristics

In the design of the equipment described in Sec. 3, we focused on the two important characteristics of the measuring instrument and considered it during the design phase.

The first characteristic is the overlap of the two measurement modes. As previously mentioned, DSPU measures the neutron count rate over a wide range using the pulse count method that measures lower count rate and the Campbell method that measures higher count rate to-

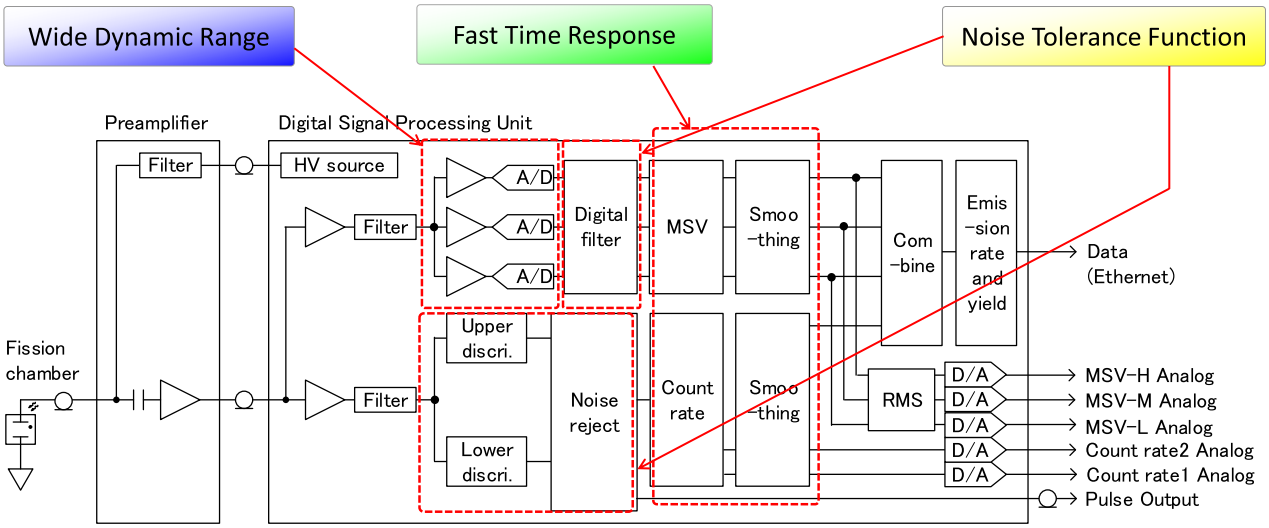

Fig. 14 Block diagram of the fission chamber signal processing.

gether. As these two are completely different methods, as described in Sec. 2.1, there is no guarantee that both measurement ranges will overlap. When the measurement ranges do not overlap, there is a problem in that not only is there a missing value in the measurement range but also the measurement value of the Campbell method cannot be calibrated. The relationship between the counting rate and the MSV voltage in the Campbell method is proportional, as shown in Eq. (1); however, it is difficult to obtain the proportional coefficient accurately by analyzing the mathematical expression.

Hence, when calibrating DSPU, it is necessary to perform experimental measurement and obtain the input/output characteristics, as shown in Fig. 15. In this input/output characteristic, it is necessary to determine a location wherein the regions where the pulse counting and Campbell methods respond linearly overlap and to determine the conversion coefficient of the Campbell method so that the slopes are equal. By determining this conversion factor, DSPU can be used as a wide-range-measuring device.

The second characteristic is the statistical error. As a high-order filter is applied to the measurement circuit of the Campbell method, it is difficult to obtain the fluctuation (statistical error) of the measured value from the characteristics of the bandpass filter.

This will be explained by considering the case of the 1st order filter as an example. The statistical error in the case of the 1st order filter can be expressed using Eq. (3) [6].

$$\frac{\sigma_s}{s(t)} = \left\{ \frac{1}{2\pi\tau(f_H + f_L)} + \frac{1}{2k\Phi\tau} \right\}^{\frac{1}{2}}, \tag{3}$$

σ_s : Statistical error
$S(t)$: Signal
τ : Time constant (s)
f_H : High cut-off frequency (Hz)
f_L : Low cut-off frequency (Hz)
k : Counting efficiency (cps/nv)
Φ : Neutron flux (nv)

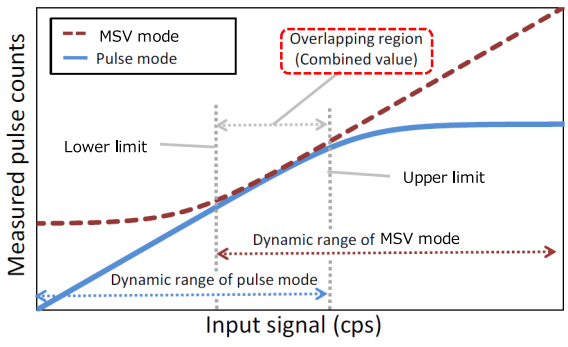

Fig. 15 Schematic diagram of the characteristics of Pulse counting and Campbell methods [2].

In this equation, the first term on the right side is the statistical error that depends on the filter circuit. The second term is the error of Poisson process. From this equation, we infer that the shorter the time constant τ, the larger the first and second terms. Moreover, the higher the filter performance, the narrower the noise bandwidth, and the first term increases. In other words, the statistical error increases in both the cases. The DSPU is designed with a short time constant because high-speed response of measured values is required, as described in Sec. 2.2. Furthermore, as mentioned in Sec. 2.3, the cutoff performance of the filter is improved. Although this equation relates to the 1st order filter, the relationship between the time constant, filter characteristics, and the statistical error is considered to be similar regardless of the order. In other words, the DSPU signal processing parameter settings may be set in a manner such that the statistical error increases. Therefore, it is necessary to ensure that the statistical error does not increase drastically.

4.2 Desktop calculation during the design stage

To confirm the overlap between the two types of measurement methods and the statistical error of the Campbell method at the design stage and to set the appropriate signal processing, a simulation model was constructed and desktop calculation was performed. The image of this simulation is shown in Fig. 16. In this simulation, similar to the actual measurement, a simulated signal that randomly generates pulse signals is prepared and input to a calculation model that simulates the DSPU signal processing function. The processing of this calculation model is similar to the signal processing circuit inside DSPU based on the input signal, and it derives the measurement result measured by DSPU through calculation. The linearity of input/output characteristics and statistical error are confirmed from the calculation results thus obtained.

For executing this method, it is necessary to create a simulated signal waveform and a calculation model that re-

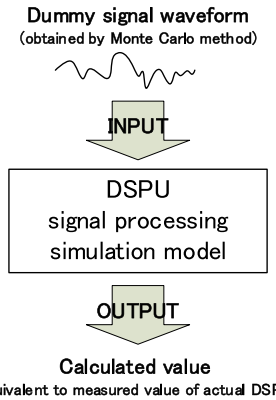

Fig. 16 Conceptual diagram of the signal processing simulation.

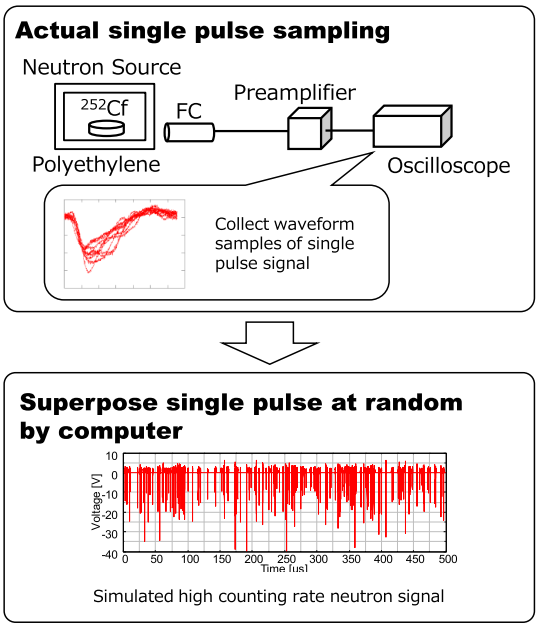

Fig. 17 Creating a dummy signal waveform.

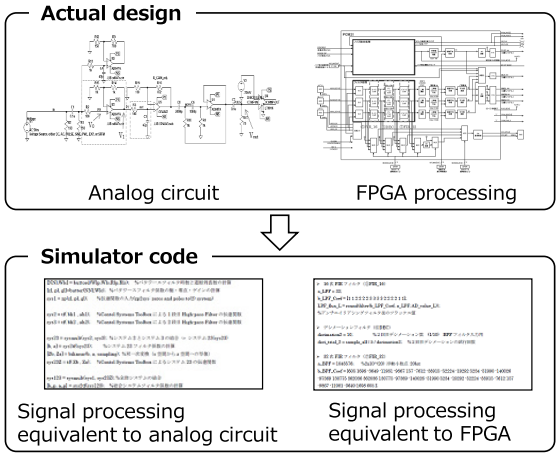

Fig. 18 Modeling the signal processing circuit.

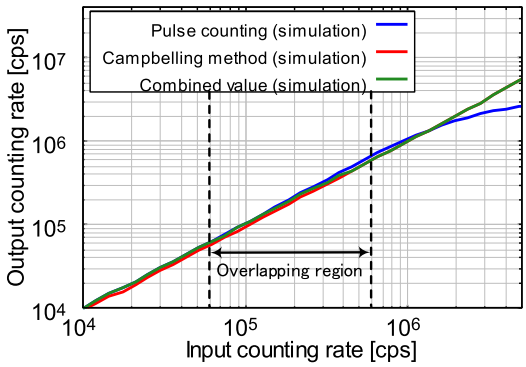

Fig. 19 Simulation result of the pulse and MSV modes.

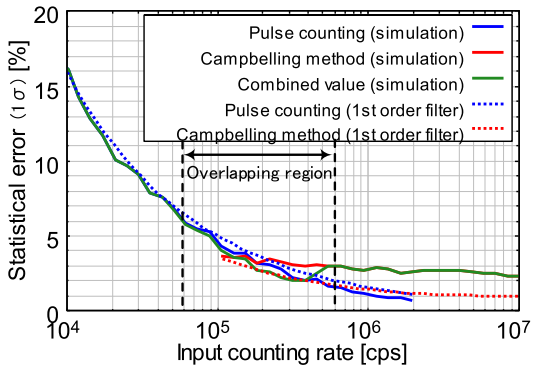

Fig. 20 Simulation result of the statistical error. Campbell mode error is twice the value of the 1st order filter.

semble the actual one. Regarding the creation of the signal waveform, as shown in Fig. 17, a lot of single-shot pulse signal waveforms are collected in an experimental system using a neutron detector and a preamplifier, and it is scattered using a software program at random times. This simulates an input signal close to the actual one, in which a pulse signal is randomly generated. Moreover, by changing the number of pulse signals to be superposed, a signal having an arbitrary intensity can be simulated. In addition, in the system of Fig. 17, approximately 40 samples were measured for a single pulse waveform.

Regarding the creation of the DSPU calculation model, a model that expresses the signal processing by the analog circuit and the digital signal processing of the FPGA in the code of GNU Octave was built, and it calculates the output value that is close to the actual measurement from the input signal waveform data. For analog circuits, a digital filter code close to it was generated based on the filter characteristics calculated using SPICE. For the FPGA, the digital filter and the mean square value calculation process described in the hardware description language (HDL) were converted to the equivalent Octave code (Fig. 18).

Using the dummy signal created in this manner and the calculation model, the linearity and statistical error were calculated on the desk and these results confirmed that there was no problem in the circuit design. Figure 19 shows the calculation results for the overlap of the two measurement methods. The blue line shows the result of calculating the output value of the pulse counting method, and the red line shows the result of the output value of the Campbell method. It shows that there was sufficient overlap in both measurement ranges.

Furthermore, the calculation result of the statistical error is shown in Fig. 20. The blue solid line shows the calculated value of the pulse method, and the red solid line shows the calculated value of the Campbell method. For comparison, the first-order lag response is shown by the dotted line of the same color. The statistical error of the Campbell method was difficult to predict in advance; however, it was found to be approximately 2.5 times worse than

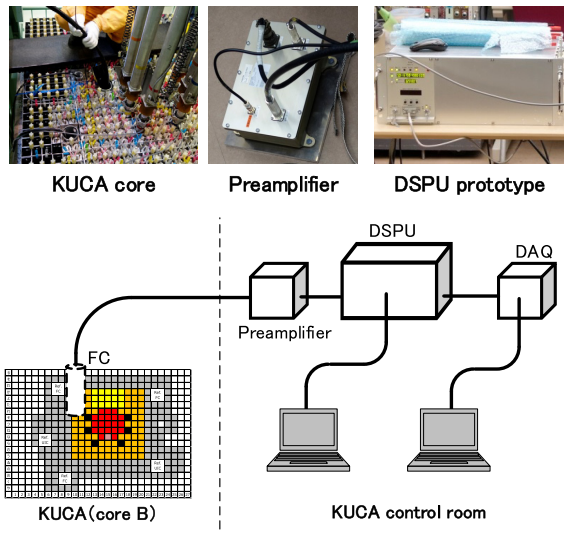

Fig. 21 Experiment system at KUCA.

that of the first-order filter. At this level, there is no problem observed in measurement.

4.3 Verification experiment at Kyoto University Critical Assembly

After manufacturing the DSPU prototype and assessing the basic functions, a verification experiment was conducted to confirm the actual neutron measurement function at the Kyoto University Critical Assembly (KUCA) experimental facility. Figure 21 shows the experimental system at KUCA. The thermal neutrons generated from the critical assembly were detected by the FC placed near the assembly and the detector signal was amplified by the preamplifier, and then the output signal of the preamplifier was measured using the DSPU prototype. The DSPU output the measurement data via UDP/IP transmission from the Ethernet port and the data acquisition device recorded this. In parallel with this, data from other detectors (i.e., FC and UIC) for the operation control of the KUCA were used as references for linearity evaluation.

As a result of this experiment, a good overlap between the two measurement methods and the statistical error of the measured values of the Campbell method were obtained. Furthermore, this result agreed with the values simulated in Sec. 4.2. The experimental results regarding overlap are shown by the black dots in Fig. 22. The horizontal axis of the figure is the count rate of signals input to the DSPU. This is obtained by multiplying the count rate value measured by the reference detector by the ratio of the count rate of FC to that of the reference detector and converting it to a value equivalent to the count rate of the DSPU. As the correlation between FC and the reference detector showed a good first-order correlation in the low count rate region of the pulse mode, the above-mentioned ratio was determined based on this result.

Next, the experimental results of statistical error are

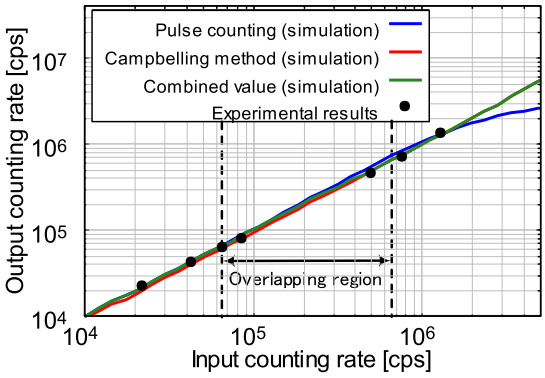

Fig. 22 Simulation and experimental result of I/O characteristics.

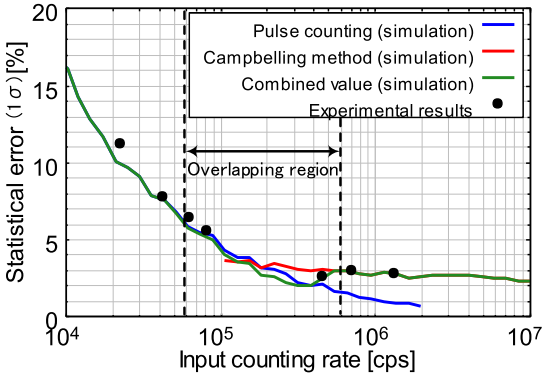

Fig. 23 Simulation and experimental results of the statistical error.

shown by the black dots in Fig. 23. This is also in good agreement with the simulation. The above-mentioned two results confirmed that the prototype of the DSPU had sufficient performance as a neutron measuring instrument in the actual neutron measurement and the calculation result through simulation.

Although not described in herein, the dynamic range of the MSV mode signal processing circuit that covered four orders of magnitude was verified via a verification test using a function generator. Consequently, it was concluded that there were no problems in the amplification characteristics of the electrical signal.

5. Installation and Operation

5.1 Entire data acquisition and monitoring system of the fission chamber

Subsequent to designing the whole measurement system for application to the fusion experiment, the production version of the DSPU and other equipment were manufactured and installed in the torus hall, basement, and measurement room of the LHD. To increase electromagnetic noise tolerance, the NFM system took every possible countermeasure during installation, including full-length cable

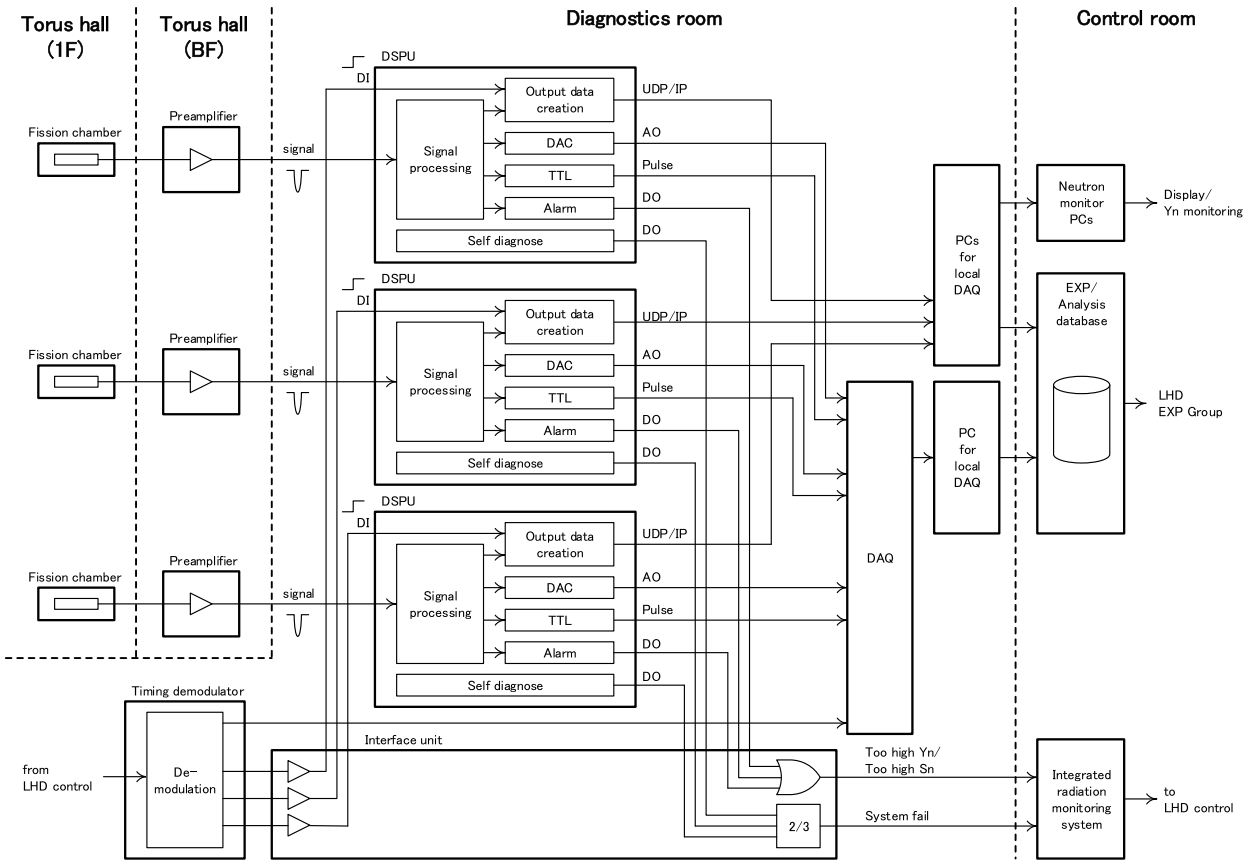

Fig. 24 Data acquisition and monitoring system of the fission chamber.

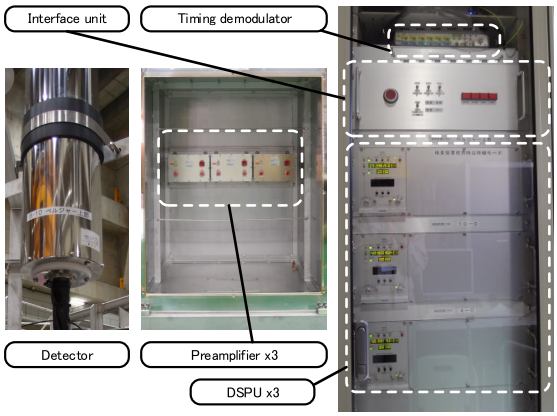

Fig. 25 Photographs of detector and signal processing equipment.

sheath, earthing, noise-cut transformer, ferrite-core, signal/grounding cable separation from power cable, EMC gaskets, and panel configuration without penetrative projection. Figure 24 shows the data acquisition and monitoring system configuration for three channels of the FC. In addition, photographs of the detector and signal processing equipment are shown in Fig. 25.

The analog output (AO) and the pulse output of the DSPU are collected by the analog input and counter function of the DAQ device, respectively. Digital data is received by a local PC for collection. All collected data are sent to the experiment/analysis database in the control room and are used by each experiment group. An experiment start signal transmitted from the control room is used for time coincidence of the data. The experiment start signal sent via the timing demodulator is divided and converted to the logic level for the DSPU and is set as a flag to the measured value of the DSPU every 0.5 ms. As the generation time of the experiment start signal is managed as a synchronization signal, the time axis of the measurement data can be determined by reading the flagged data.

As a monitoring function, the S_n and total neutron emission yield are monitored. Each DSPU has an alarm assessment function and constantly monitors the rate and yield. If an alarm is activated in any one of the three channels, it is immediately transmitted to the control room.

5.2 Assessing neutron detection function

Subsequent to the installation of the entire system was completed, the soundness of the neutron detection function was confirmed using a neutron source. Specifically, a ^{252}Cf neutron source was placed near the detector and the integrated pulse height distribution was measured. The integrated pulse height distribution is a characteristic obtained by measuring the count rate while stepwise changing the

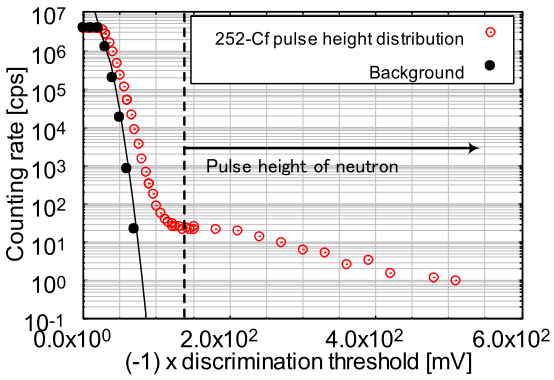

Fig. 26 Integral pulse height distribution.

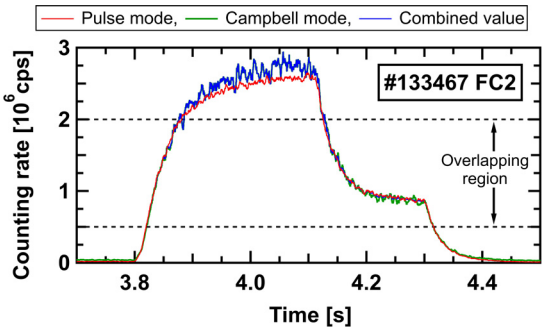

Fig. 27 Example of the time evolution of the count rate when adjusting the Campbell sensitivity.

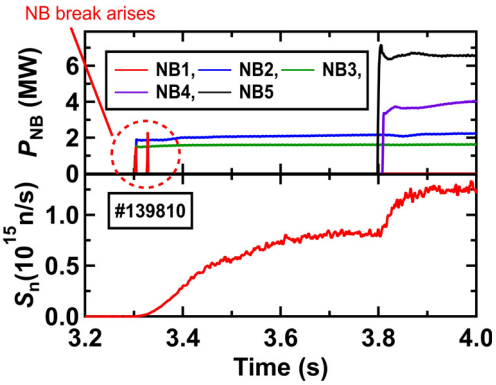

Fig. 28 Example of measurements when an NB-break occurs. There is no influence on the total neutron emission rate (S_n).

threshold voltage of the pulse mode discriminator. In the low threshold voltage region, counting by noise is dominant; therefore, it does not serve as information for confirming the neutron detection function. However, even in the high threshold voltage region, if a certain level of count rate is maintained, it can be said that this system can detect neutrons. This is attributed to the neutron detection signal being larger than other signals such as electrical noise and gamma rays and the signals are counted even if the threshold voltage is high to some extent.

Figure 26 shows the actual measurement results. In this figure, the values measured without the radiation source are indicated by black circles and the measurement results with the radiation source placed are indicated by red circles. When the radiation source is placed, counting by the signal with a large pulse height is clear in the region where the threshold voltage is approximately 120 mV or greater. Consequently, there is no problem in the neutron detection function. In this result, although the characteristics of the region where the threshold voltage is low are slightly different, it is considered that the background was changed owing to the shield around the detector being opened because the radiation source was placed near the detector.

5.3 Neutron measurement in D-D experiments

To calibrate the equipment, the conversion factor of S_n and counting rate was obtained by in situ calibration experiment using a neutron source [7,8]. Further, the calibration of the device was completed by determining the conversion factor of the counting rate and the measured value of the Campbell mode. Subsequently, this system started operation for D-D experiments.

Figure 27 is an example of an actual measurement. The red, green, and blue lines are the pulse mode, the Campbell mode, and the combined values of both, respectively. Both the pulse and Campbell modes are in good agreement in the overlapping region. In the region that is beyond the overlapping region, there is a difference between the pulse and MSV, which is attributed to the pulse mode losing its linearity owing to saturation.

Moreover, in the D-D experiments so far, the S_n is able to be measured without any serious problems even when at the occurrence of an NB break. Figure 28 shows an example of this. The upper figure shows the power of the NB injector, and the lower figure is a graph showing the measured S_n. At the point of approximately 3.3 s in this graph, the NB's power went down and this implied that an NB break occurred; however, there was no disturbance in the measured values that could be influenced by this break. If they were affected by this noise, an unnatural waveform should appear so that the measured value suddenly changed.

Finally, as a result of applying the NFM system to the D-D experiment, Fig. 29 shows an example of performing the NB-blip experiment introduced in Sec. 2.2 in LHD. As shown in the middle row of the figure, a short-pulse NB was injected in succession from NB1 (co-passing injection), NB2 (counter-passing injection), NB3 (co-passing injection), and NB4 (perpendicular injection). The central electron temperature T_{e0} and the line averaged electron density n_{e_ave} are shown in the top row. The lower part shows the neutron emission rate, which shows the re-

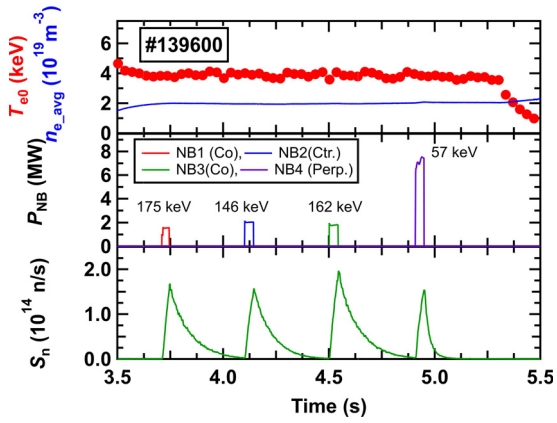

Fig. 29 Example of an actual NB-blip experiment using the neutron flux monitoring system.

sponse of each NB. These pulse responses have a rise time constant of approximately 50 ms and a fall time constant of approximately 80 ms. The DSPU has a sufficiently fast time response to these time scales in a manner such that the responsiveness of the device does not blunt the waveform. K. Ogawa *et al*. have shown that these response characteristics are in good agreement with the simulation performed using FBURN, GNET [9, 10].

6. Conclusion

To measure the dynamic and abruptly changing S_n in fusion experiments, such as the D-D experiment at the LHD, a neutron measuring equipment with the following three features was developed.

(i) Wide dynamic range
(ii) Fast time response
(iii) Sufficient noise tolerance

In particular, it was an unprecedented attempt in terms of mounting a noise tolerance function that applies digital signal processing, focusing on its vulnerability to noise owing to high-speed response.

After designing the important characteristics by applying simulation, the neutron measurement function was demonstrated in the nuclear reactor. Subsequently, the product version of three systems was installed in the LHD, and the experimental operation was started successfully. Furthermore, impressive results regarding fast ion confinement have been achieved thus far. Through the experimental operation in the LHD, it has been proved that this device effectively functions in the fusion experiments. In the future, we will aim to apply it to other experimental devices and further improve its functions.

Acknowledgments

This work was supported by the National Institute for Fusion Science (NIFS) and National Institute of Natural Sciences, Japan. Testing at the KUCA was supported partly by the Institute for Integrated Radiation and Nuclear Science, Kyoto University, Japan.

[1] Y. Endo *et al*., IEEE Trans. Nucl. Sci. NS-29, No. 1, 714 (1982).
[2] T. Hayashi *et al*., Rev. Sci. Instrum. **75**, 3375 (2004).
[3] K. Tobita *et al*., Nucl. Fusion **34**, No. 8, 1097 (1994).
[4] M. Osakabe *et al*., Fusion Sci. Technol. **72**, 199 (2017).
[5] M. Isobe *et al*., Rev. Sci. Instrum. **85**, 11E114 (2014).
[6] R.A. DuBridge, IEEE Trans. Nucl. Sci. **14**[1], 241 (1967).
[7] T. Nishitani *et al*., Fusion Eng. Des. **136**A, 210 (2018).
[8] M. Isobe *et al*., IEEE Trans. Nucl. Sci. **46**, No. 6, 2050 (2018).
[9] K. Ogawa *et al*., Nucl. Fusion **59**, 076017 (2019).
[10] K. Ogawa *et al*., Plasma Phys. Control. Fusion **60**, 095010 (2018).